NAL TR-687T

ISSN 0389-4010
UDC 629.735.014.16:
629.7.025.35:
534.2

TECHNICAL REPORT OF NATIONAL AEROSPACE LABORATORY

TR-687T

Aerodynamic Noise Generated by Jet-Wing/Flap Interactions of the External USB Configuration of STOL Aircraft

[II] Full-Scale Model Experiment Using FJR710 Turbofan Engine

Masataka MAITA
Tadao TORISAKI
Katsumi TAKEDA
Shigemi SHINDO
Mitsuo MORITA
Shizuo SEKINE
Shin NAKAYAMA
Akira YOSHIDA
Hiroshi KONDO
Masakatsu MATSUKI

October 1981

NATIONAL AEROSPACE LABORATORY

CHŌFU, TOKYO, JAPAN

Aerodynamic Noise Generated by Jet-Wing Flap Interactions of the External USB Configuration of STOL Aircraft

[II] Full-Scale Model Experiment Using FJR710 Turbofan Engine

Masataka MAITA*, Tadao TORISAKI*, Katsumi TAKEDA*,
Shigemi SHINDO*, Mitsuo MORITA**, Shizuo SEKINE**,
Shin NAKAYAMA**, Akira YOSHIDA**, Hiroshi KONDO**,
and Masakatsu MATSUKI**

ABSTRACT

Acoustic characteristics of the external upper surface blowing (USB) concept of a propulsive-lift configuration were studied by full-scale model static experiments. Test components included an FJR710 turbofan engine with an acoustically treated nacelle and a USB wing/flap assembly. These were utilized in conjunction with the ground verification testing of the propulsive systems of the National Aerospace Laboratory Quiet STOL Research Aircraft. Results were compared with the previous 8%-scale cold flow model data. The deffect of shielding provided by the wing/flap surface on aft-radiated turbofan engine noise was studied and some attempts were made to reduce USB noise.

概　　要

本論文は，USB 方式 STOL 機高揚力システムからの騒音特性，発生／伝播メカニズムの解明及び騒音低減化技術の確立のための技術研究の一環として，FJR 710 ターボファンエンジンを用いた実機スケールの USB 方式高揚力システム・モデル試験による解析結果を議論するものである。高揚力システムからの騒音の主要音源の identification，遠距離場に伝播する騒音レベル及び周波数特性についてのデータスケーリング法，USB 形態に於ける翼によるエンジン騒音の遮蔽効果等について明らかにし，又高揚力システムからの騒音低減化のための一つとして，サイド・フェンス方式に因る試みを行った。

NOMENCLATURE

AR_e Nozzle aspect ratio defind as nozzle area divided by the square of nozzle height h, Area/h^2

β_u Nozzle kickdown angle, angle between horizontal and top surface internal leaving angle, [deg.]

δ_f USB flap deflection angle, [deg.]

f_{peak} The frequency corresponding to the maximum SPL in acoustic spectrum.

S_t Strouhal number based upon the wall jet thickness at the flap trailing edge δ.

* Noise and Emission Research Group
** Aeroengine Division

N_1	FJR engine fan rotor speed, [rpm]
FMM	Flush Mounted Microphone
V. G.	Vortex Generators, the flow attachment device.
U_{jet} (U)	The mean jet exhaust velocity at USB nozzle exit, [m/s]
F−90°, F+90°	Far-field microphone location at Flyover Plane −90° or +90° (the direction directly below or above the wing respectively), of distance 25-meter from engine nozzle centerline.
PNL	Perceived Noise Level, [dB]
OASPL	Overall Sound Pressure Level, [dB]

INTRODUCTION

Recently research and development programs of Short Takeoff and Landing [STOL] Aircrafts, which are considered as one of the candidates for transports in the late 1990s, have been promoted. Typical examples are Quiet Fanjet STOL Aircraft Research program of National Aerospace Laboratory, Japan or YC-14 and Quiet STOL Research Aircraft [QSRA] programs of National Aeronautics and Space Administration, USA.

The external Upper Surface Blowing [USB] is the primary concept in achieving powered high lift for these STOL Aircraft applications. The powered lift augmentation during Takeoff and Landing required for STOL operations is derived by deflecting turbofan engine exhaust jet adjacent to the wing and flap upper surface by a Coanda principle, i.e. enhancement of the lift-production capabilities of the total lifting systems by a direct deflected thrust vector and by powered circulations.

From a commutity noise point of view, short-haul transports employing this design concept will make it possible to operate from short runways with highly maneuvable, steep and curved flight paths, and the installations of turbofan engines over the wing shield some of aft-radiated engine noise, which then result in reduced community noise and its exposure.

However, the external upper surface blowing flap produces an additional noise because engine exhaust flow interacts with wing and flap surfaces. In order to meet the stringent noise goals which are being put forth and to meet a community acceptance, noise reduction technologies must be developed.

While the state of art on this subject is advancing, the details of the actual noise generating and radiation mechanisms were not known. These noise generation mechanisms are primarily due to turbulences, of either entropy or vorticity modes in the noise sources.

The research progran has been undertaken to study the acoustic characteristics of the USB propulsive-lift configuration using the FJR710 turbofan engine[1] and full-scale USB wing/flap assembly model of the NAL Quiet STOL Research Aircraft (cf. Appendix II). The full-scale acoustic tests were part of a technology integration program to accomplish initial full-scale engine ground verification testing and to measure the aero-acoustic and thermal wing/flap load environment in order to assess the acoustic fatigue failure of structural members and propulsive-lift performance. The acoustic content included the noise directivity pattern, noise spectra for various USB flap configurations and engine power rates, coherence data between the fluctuating surface pressure and the far-field noise, noise dependence on engine exhaust jet velocity, the engine noise shielding effect of the wing/flap surface, and a determination of the effect of engine exhaust flow attachment devices on noise generation. Based upon the noise data and the morphology of the basic theoretical studies, noise generation mechanisms and noise source identification related to the USB powered-lift system are also discussed.

In the present paper, we attempt to summarize the principal results and conclusions of acoustic characteristics of USB propulsive-lift configuration full-scale model using FJR710

Turbofan engine.

APPARATUS AND PROCEDURE

The typical setup of the external upper surface blowing propulsive-lift configuration is shown in photograph 1. The model was powered by an FJR710 Turbofan engine, which had a bypass ratio of 6.5, rated at approximately 4900kg static thrust.

Acoustically treated nacelle inlet equipped with a bellmouth was installed to the fan inlet (cf. Photograph 2). FJR710 Turbofan engine

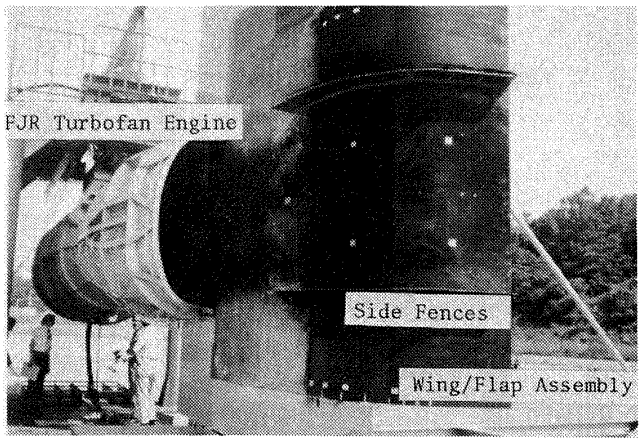

Photograph 1 Typical model configuration with Side Fences installed ($\delta_f = 60^\circ$)

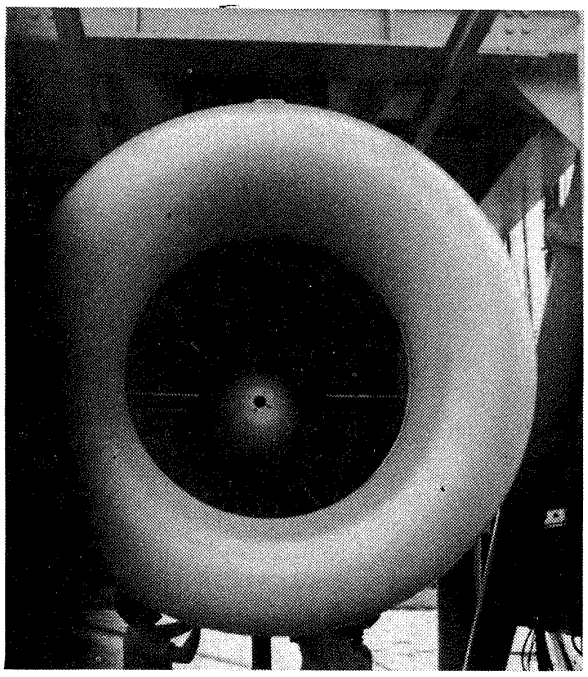

Photograph 2 Acoustically treated nacelle inlet equipped with a bell-mouth

was equipped with the AR_e of 2.66 (the aspect-ratio defined as nozzle exit area divided by the square of nozzle maximum height) D-shaped nozzle directed downward toward the top of the main wing. The D-nozzle kickdown angle β_u (cf., Nomencrature) was 22°. The wing had double USB flaps. For landing flap configuration ($\delta_f = 60^\circ$), apparatuses for enhancing Coanda flow attachment were employed such as Side fences or Vortex generators, to prevent engine exhaust flow separation over USB flaps.

The present USB propulsive-lift configuration simulated the outboard engine propulsive content of NAL Quiet Research Air craft. A sketch of the geometry of the engine-wing/flap assembly is presented in Figure 1.

The test were conducted at National Aerospace Laboratory-Kakuda branch outdoor test facilities.

Main test parameter variations related to the acoustic measurements were:

[I] Engine power setting
[II] USB flap deployment angles $\delta_f = 0^\circ$, 30° and 60° representing Cruise, Takeoff and Landing USB flap configuration respectively. (cf. Photographs 3)
[III] Installation and/or retraction of engine exhaust flow attachment device on the wing/flaps.

Far-field noise data were taken for all parameter variations by 1/2-inch B and K condenser microphones placed on a 25-meter radius centered on the intersection of the exhaust nozzle plane with the engine exhaust nozzle centerline, which was 2.5 meter above the ground and the microphones were elevated on poles to be the same horizontal plane as the engine centerline.

The surface fluctuating pressures measured by 1/4-inch B and K condenser microphones which were flush-mounted on the wing and USB flap upper surface with teflon-coated adaptors (cf. Photograph 4), and ensured that flat frequency

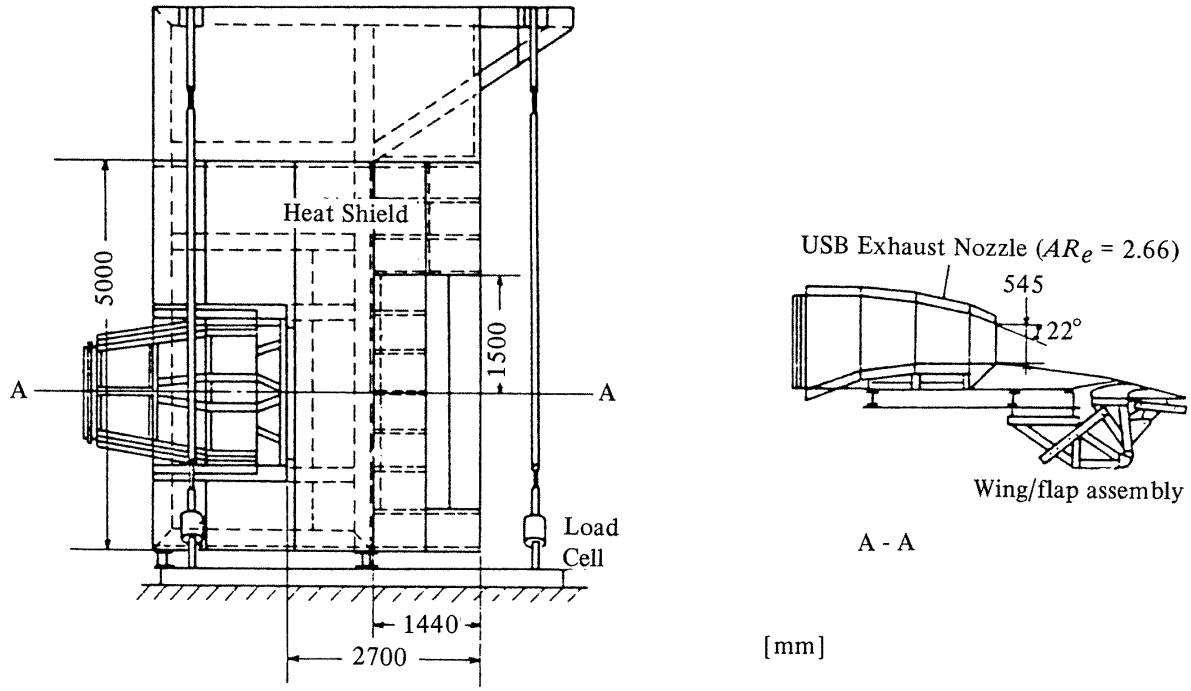

Figure 1 A sketch of the geometry of FJR710 engine wing and flap assembly

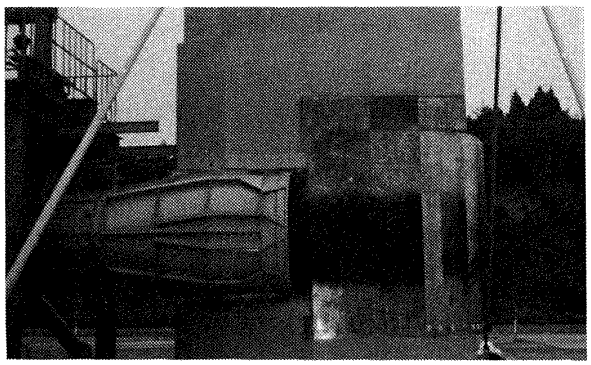

Landing Flap Configuration without any special devices, $\delta_f = 60^\circ$

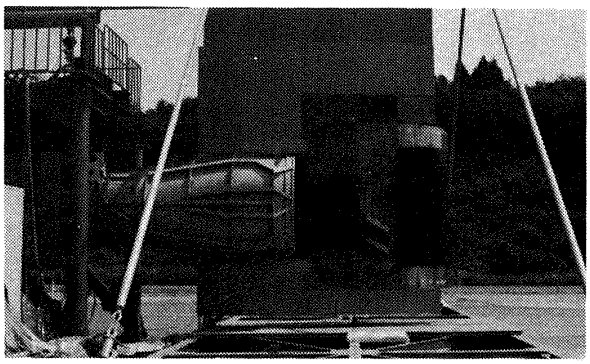

Landing Flap Configuration with Voltex Generators installed, $\delta_f = 60^\circ$

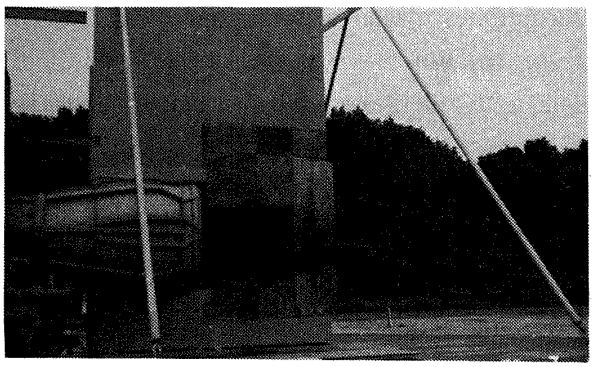

Takeoff Flap Configuration, $\delta_f = 30^\circ$

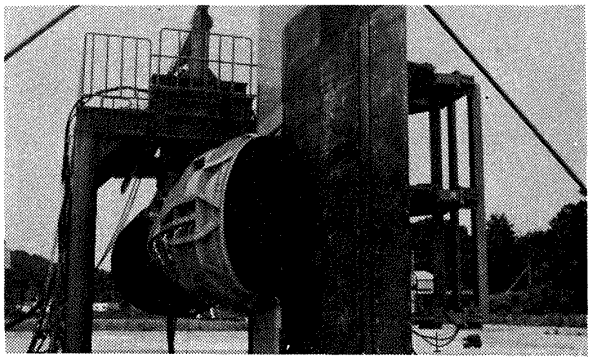

Cruise Flap Configuration, $\delta_f = 0^\circ$

Photographs 3 USB Flap Configurations

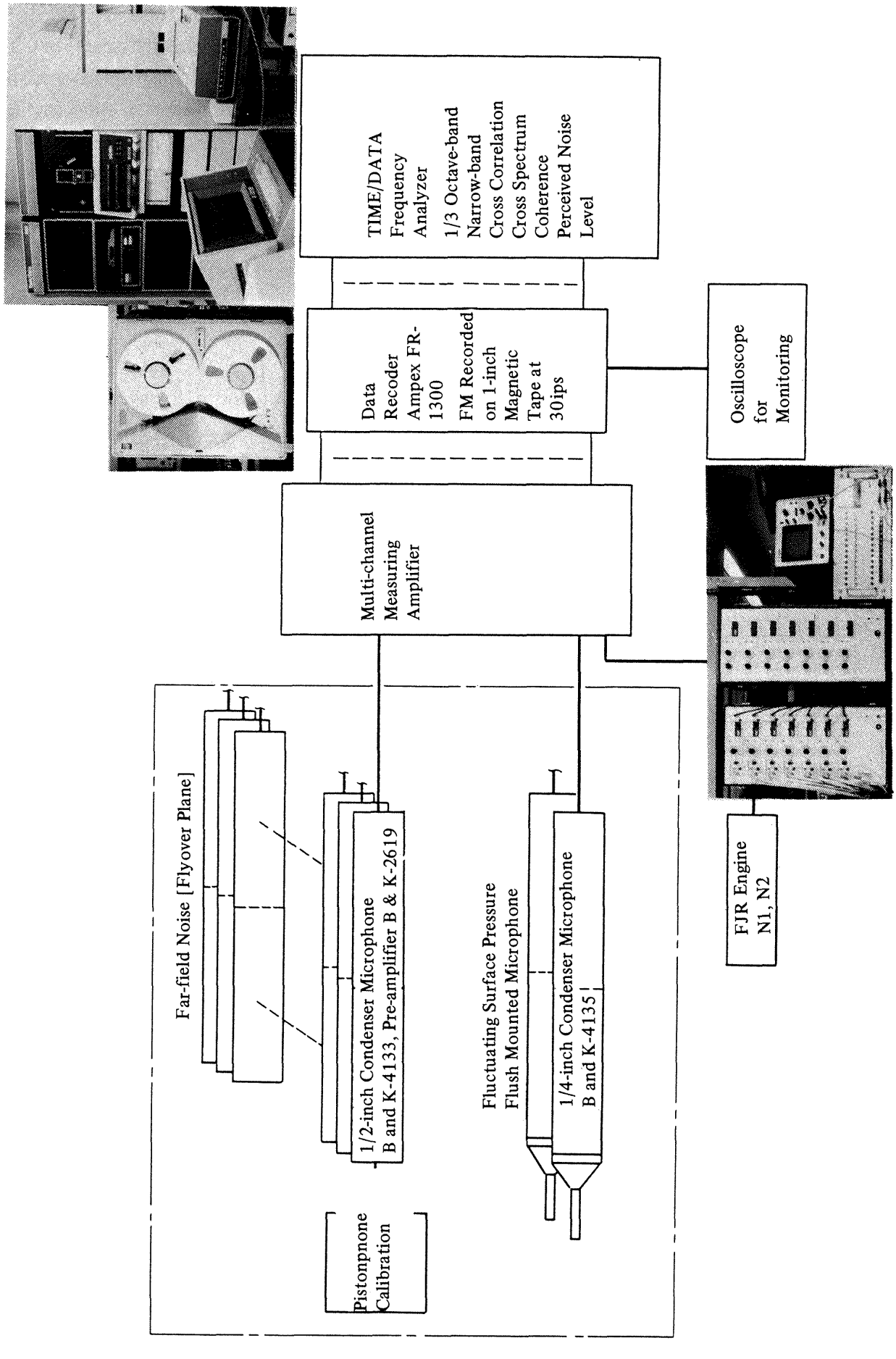

Figure 2 A schematic diagram of data analysis

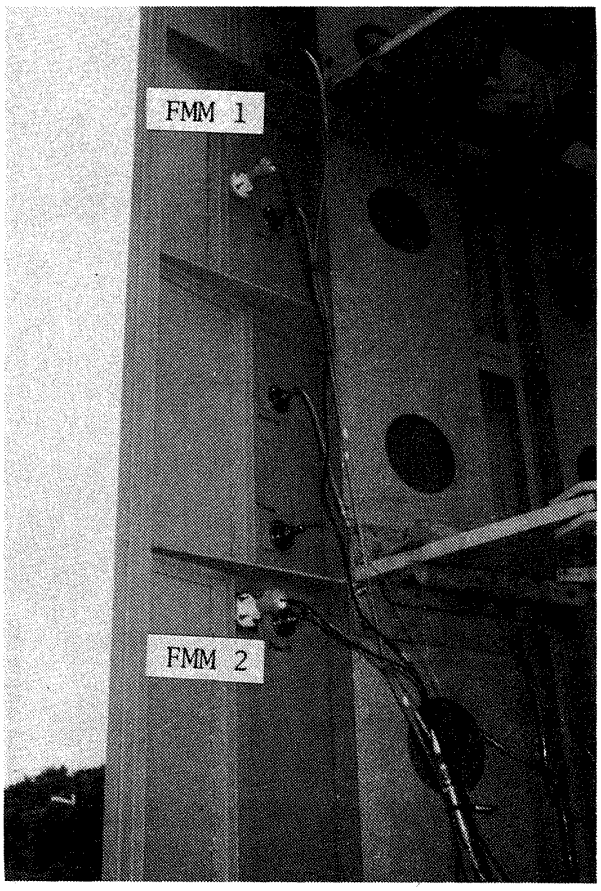

Photograph 4 Flush mounted microphones with teflon-coated adaptor

response within ±0.5 dB up to 10kHz[2] over the environment temperature range up to 150°C.

Noise data were FM recorded on a Data Recorder at tape speed 30ips. Data acquisition and reduction were the same as illustrated schematically in Figure 2.

No corrections were applied to compensate for the ground reflection interference in the noise data.

In addition to the acoustic measurement, extensive instrumentations of FJR710 Engine and other USB environment were incorporated, which provided for lift force to engine thrust, wing and flap surface static pressure profiles, surface temperature profiles together with engine performances.

RESULTS AND DISCUSSION

1/3 Octave-band SPL spectra of Cruise (δ_f=0°), Takeoff (δ_f=30°) and Landing (δ_f=60°) USB flap configurations for the case of 40% engine thrust setting at microphone position Flyover Plane –90°, corresponding to directly beneath the wing, is presented in Figure 3, comparing with the spectrum of FJR engine alone as a baseline case. The high-frequency (above 2000 Hz) activities, predominated for the engine alone case, is mainly contributed by Fan generated noise.

Exhaust jet noise for FJR engine alone has been estimated[3] to have the peak frequency around 160Hz and is not predominant in this case. The additions of the USB wing/flap system result in a noise increase for the lower frequencies in the spectrum, while in the high-frequency ranges, SPL is decreased by the shielding effect of wing/flap surface. Based upon past studies[4]-[25], noise from the external USB configuration is qualitatively categorized in Figure 5 and basic theoretical formulations are summarized in Appendix I.

The low-frequency activities (around 100Hz) in the spectra of USB system noise are the principal contribution of exhaust jet wing/flap surface interations.

The effect of exhaust jet velocity variation on the USB propulsive-lift noise SPL, for cruise flap configuration, as an example at the Flyover Plane –90° microphone position is presented in Figure 6. In the figure, the peak SPL frequency f_{peak} changes approximately under the constant Strouhal number.

Overall sound pressure level (OASPL) from the Cruise and Takeoff flap USB system configurations vary with the exhaust jet velocity according to approximately 5th-power law dependence at Flyover Plane –90° direction as shown in Figure 7 and Figure 8 respectively, which confirmed that the edge noise being predominant noise source can be estimated from

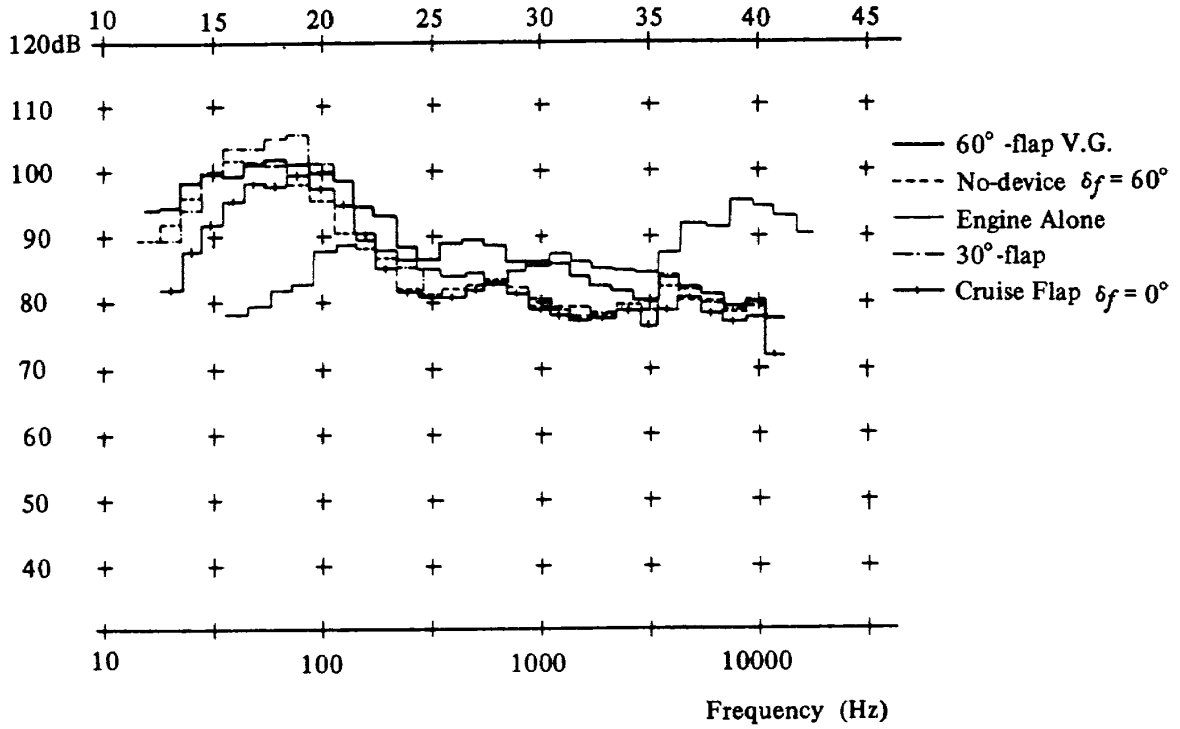

Microphone Flyover Plane–90°
Engine 40% Thrust

Figure 3 1/3 Octave-band SPL spectra of various USB flap configurations at the direction below the wing (Flyover–90°)

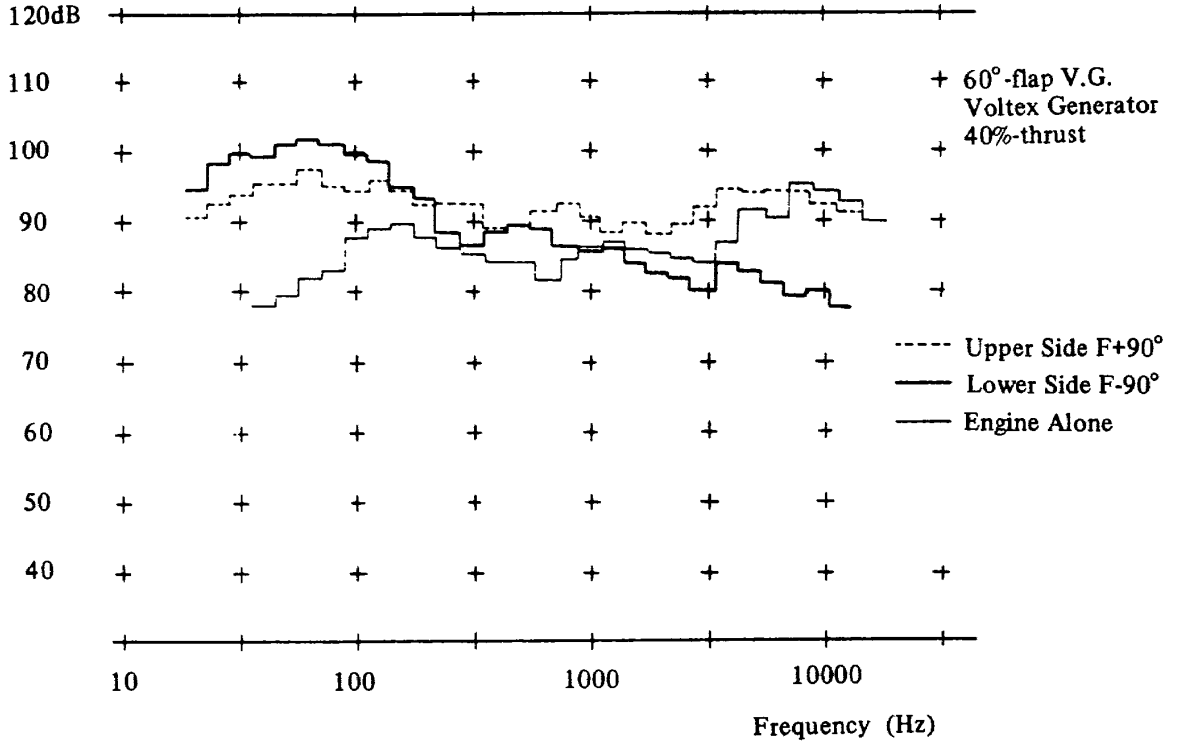

Microphone Flyover Plane ±90°
(Distance 25m from Engine Exhaust Nozzle Exit Center)

Figure 4 Effect of engine noise shielding by wing and flap surface

Jet Mixing/Wall Jet Mixing Noise [Category II]

Jet before impinging to Wing/Flap Surface/Wall Jet Resulting from the fluctuating stresses in flow Quadrupole in nature. U^8-dependence.

Entropy Noise [Category I]

Due to unsteady thermal diffusion from heated Wing/Flap surface. U^4-dependence.

Jet Scrubbing Noise [Category III]

Induced fluctuating pressure on the Wing/Flap surface adjucent to turbulent boundary layer. Dipole in nature. U^6-dependence.

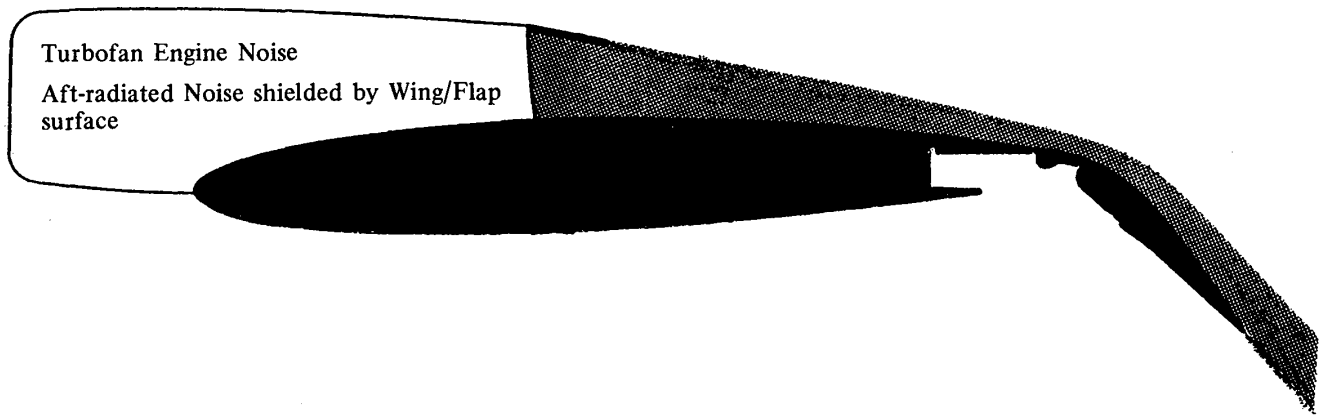

Trailing Edge Noise [Category IV]

The predominant noise source at the direction below Wing/Flap. Quadrupole in nature. U^5-dependence. Directivity single-lobe pattern $\cos^2[\theta/2]$, θ angle from the forward direction. Due to the amplification of turbulence near the trailing edge.

Figure 5 Summary of USB Noise

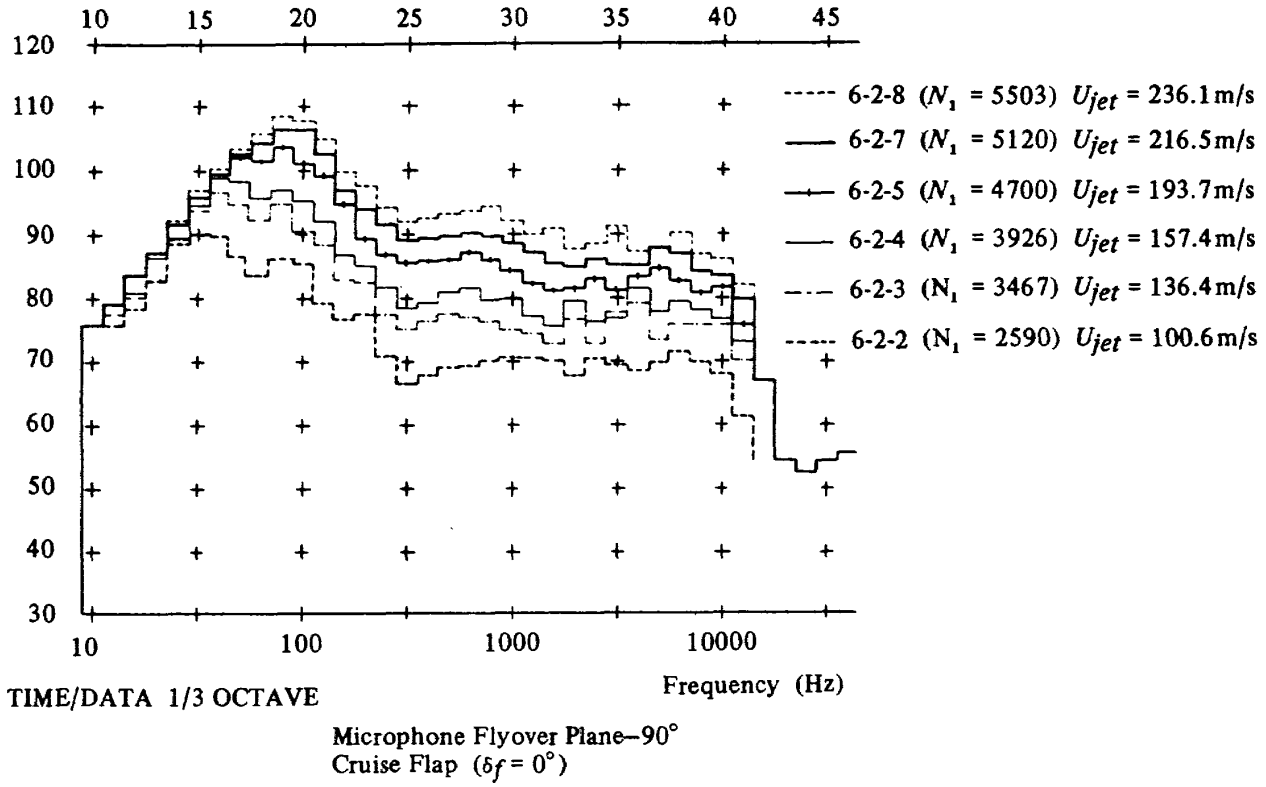

Figure 6 Effect of exhaust jet velocity variations on USB noise SPL spectra for cruise flap configuration

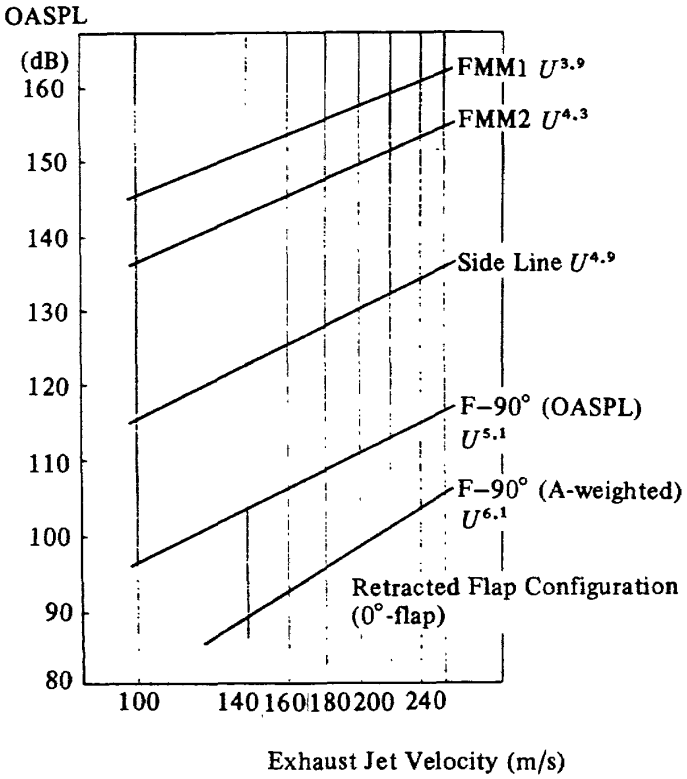

Figure 7 Overall sound pressure level (OASPL) dependence on exhaust velocity for cruise flap configuration

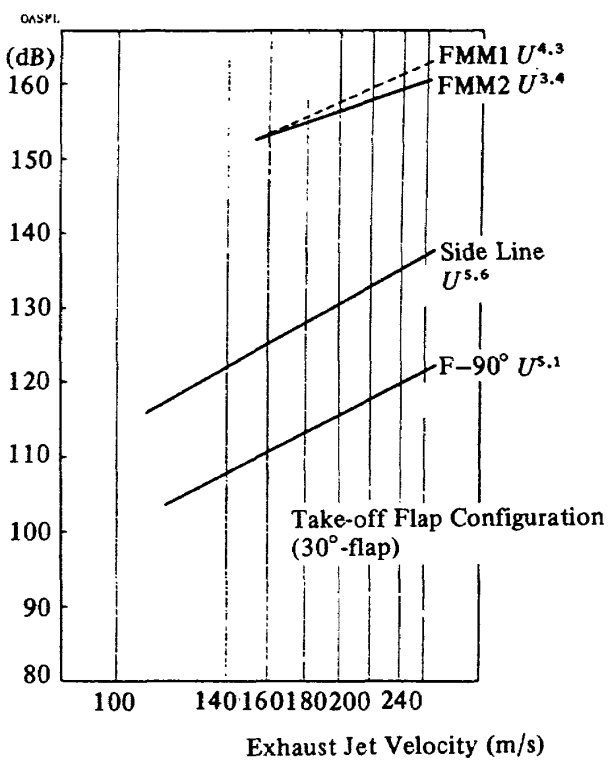

Figure 8 Overall sound pressure level dependence on exhaust velocity for takeoff flap configuration δ_f = 30°

Ffowcs Williams et al.[4] 's Scattering Half-edge analysis in the present case. (cf. Appendix I) (However, for a certain flow field where the velocity gradient beneath the jet being very high and highly unstable and large-scale flow instabilitites being excited, some modifications to Ffowcs Williams et al.'s arguments would be necessary as have been pointed out by Tam[5] or Paterson[6] et al.)

Noise generated from the USB propulsive-lift configuration differs in its fundamental aeroacoustic mechanisms which depend upon its configuration geometries. Now for the cruise flap configuration ($\delta_f = 0°$), the surface dipole noise (Category III) is assumed to be negligible since as have discussed, the strength of surface dipole is approximated to be equal to the fluctuating viscous stress. And the plane surface would act merely to reflect the volume quadrupole and hence at the direction below the surface noise generated by Category II would not be contributive to OASPL and also the engine internal noise being shielded by the wing/flap surface, Edge interaction noise (Category IV) will be the only remaining contributive noise at the direction Flyover Plane –90°. Granted that these arguments hold for the Cruise flap configuration, OASPL dominated by Category IV edge interaction noise will be demanded to have closely the 5th-power law dependence of U_{jet}.

1/3 Octave-band spectra of fluctuating pressure at Flush Mounted Microphone 1 in the vicinity of the main flap trailing edge (cf. Figure 10) for 90% thrust engine power setting is shown in Figure 9 where its peak SPL frequency range corresponds to the f_{peak} of the far-field noise spectrum.

Series of coherence data between the fluctuating surface pressure and the far-field noise at Flyover Plane –90° direction were taken and found to be the same tendencies as in the 8%-scale cold flow model experiment, i.e. the flap

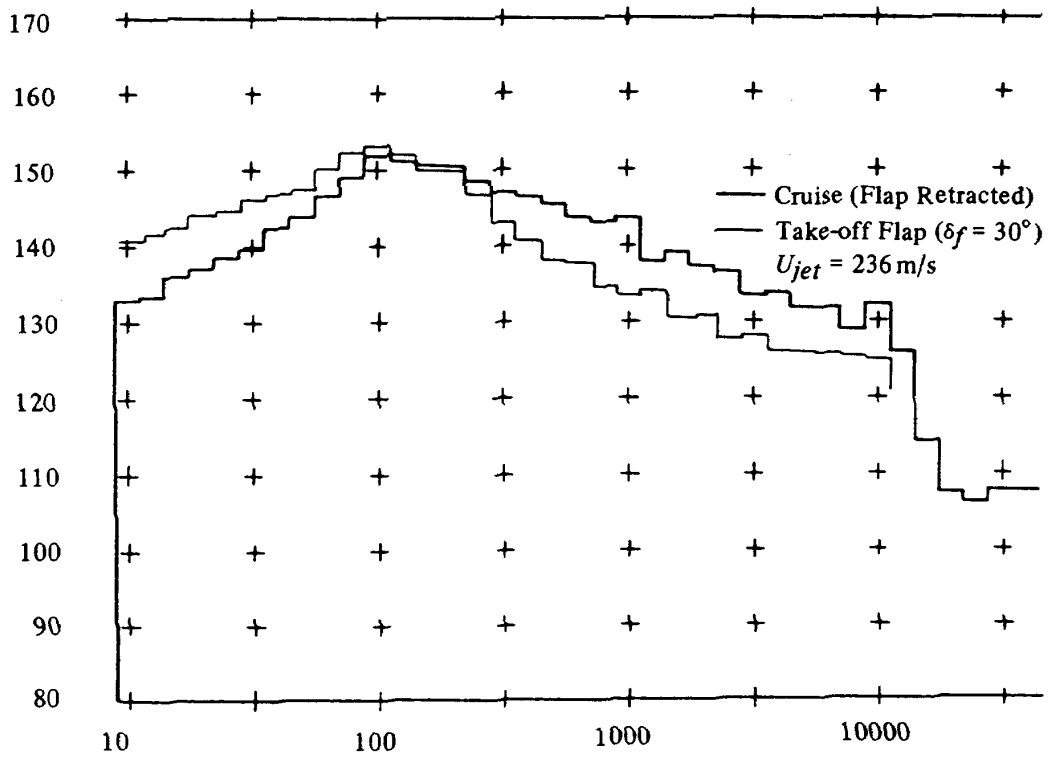

Figure 9 1/3 Octave-band spectra at flush mounted mic 1

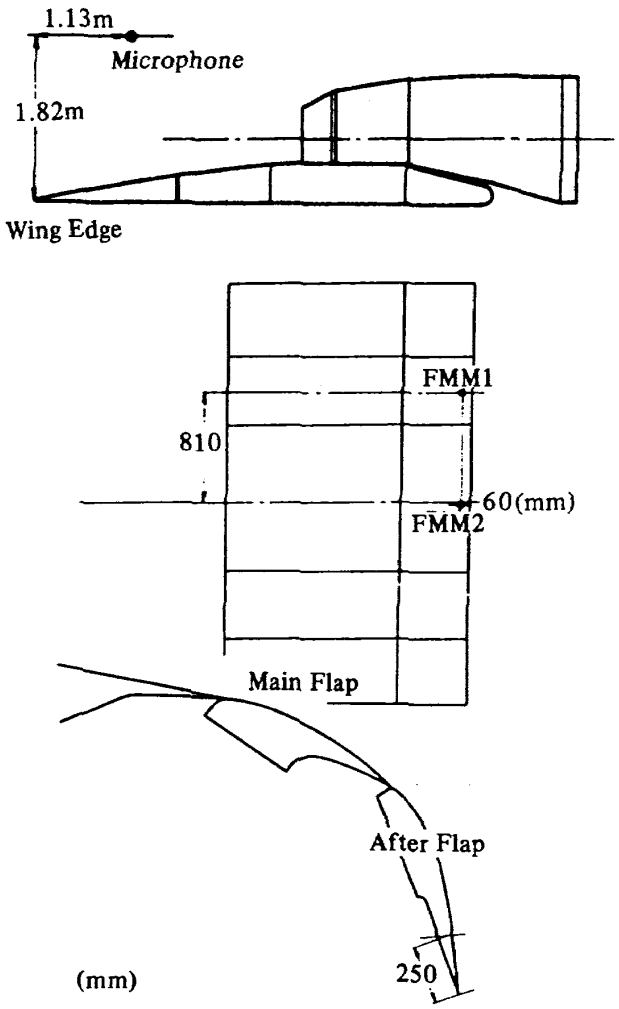

Figure 10 Location of Flush Mounted Microphone 1, 2

trailing edge was the highest magnitude of coherence location. (cf. Figure 9 for the example)

Figure 12 shows the normalized SPL spectral density using Strouhal number. For both 8%-scale cold flow models[25] and full-scale propulsive-lift systems ($\delta_f = 30°$ Takeoff flap), the Strouhal number corresponding to each spectral peak frequency range is approximately constant at 0.05 and the normalized SPL spectra have similarity in form in the peak SPL level Strouhal number range and scatter outside these ranges.

The preceeding results imply that these edge-interaction noise is essentially independent of jet upstream sources, i.e. whether compressed air jet or turbofan engine exhaust jet. And Strouhal normalization suggests that the low-frequency noise from actual USB propulsive-lift configurations can be predicted well from the small-scale cold flow model experiments.

In the Figure of 13, the comparison of noise spectra from the USB propulsive system in the directions perpendicular to the flap trailing edge below and above the wing/flap (lower and upper sides of the Figure respectively) is shown. In the high-frequency ranges, the sound levels below the

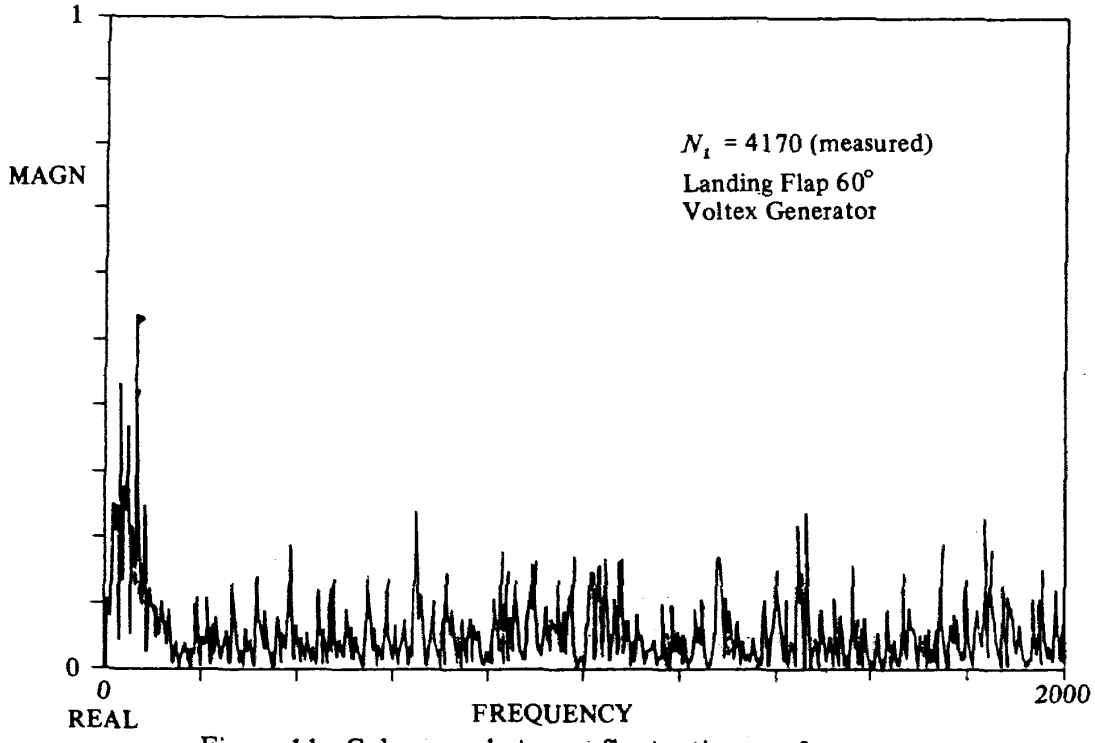

Figure 11 Coherence between fluctuating surface pressure and far-field noise at Flyover −90° direction

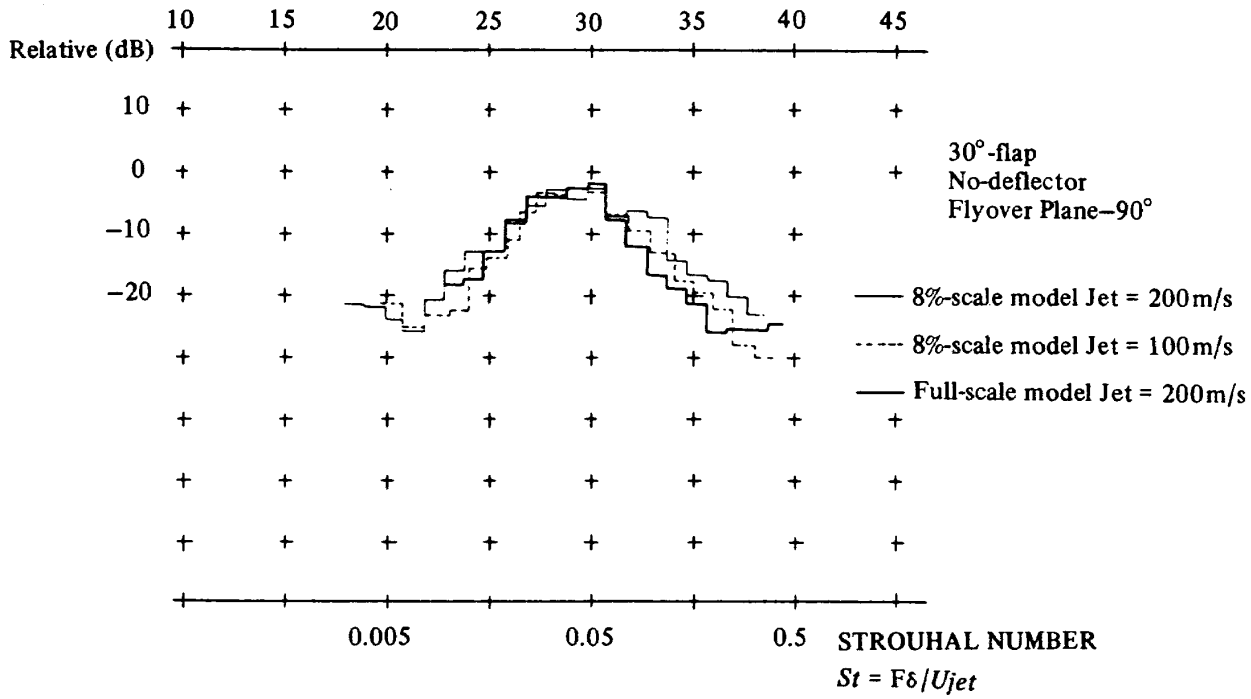

Figure 12 The normalized SPL spectral density using Strouhal number at the direction Flyover −90° for takeoff flap configuration $\delta_f = 30°$

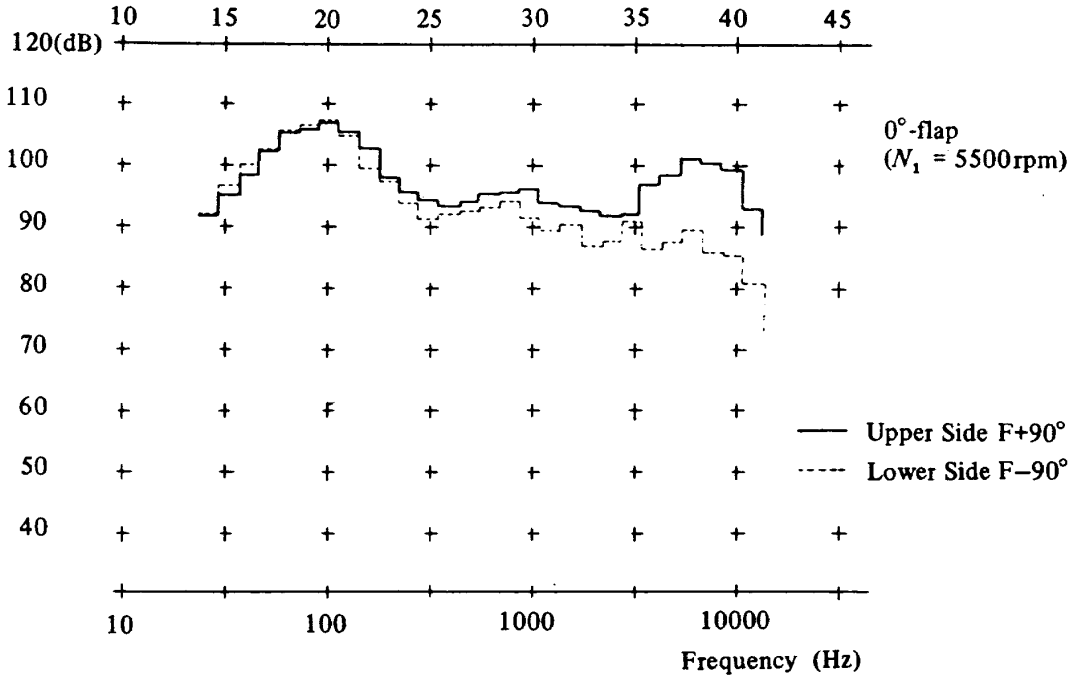

Figure 13 Comparison of USB noise SPL spectra in the directions perpendicular to flap trailing edge below and above the wing

wing are less than the levels above the wing due to the shielding effect by the wing/flap surface and both peak level frequency ranges lie in the same frequency band in low-frequency ranges and their peak SPL intensities are of the same order magnitude. The above results are possible since as we have discussed before the predominant noise source contributing to the peak SPL frequency ranges is located near the flap trailing edge where the least noise shielding by wing/flap occurs.

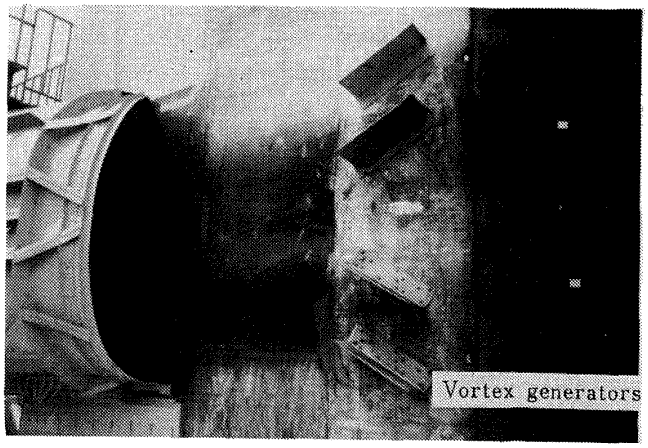

Figure 14 A photograph of Voltex Generators installed on wing with incidence angle of 30° to engine centerline

When the Vortex Generators were installed on the wing surface in order to enhance the engine exhaust flow attachment for the landing flap configuration ($\delta_f = 60°$) (cf. Figure 14), the associated jet vortex phenomenon will generate additional noise. 1/3 Octave-band spectra at the far-field Flyover Plane –90° direction and at the flap trailing edge (Flush Mounted Microphone FMM2) for the landing flap configuration with/without Vortex Generators are presented in Figure 3 and Figure 15 respectively.

In the mid-frequency ranges (around 500Hz), increases in noise spectral levels to be about 6-10dB were resulted in. And with the Vortex Generators installed, exhaust velocity dependence on OASPL at the Flyover Plane –90° direction was 6th power law approximately, while with the retraction of Vortex Generators resulted in lower power dependence as shown in Figure 16.

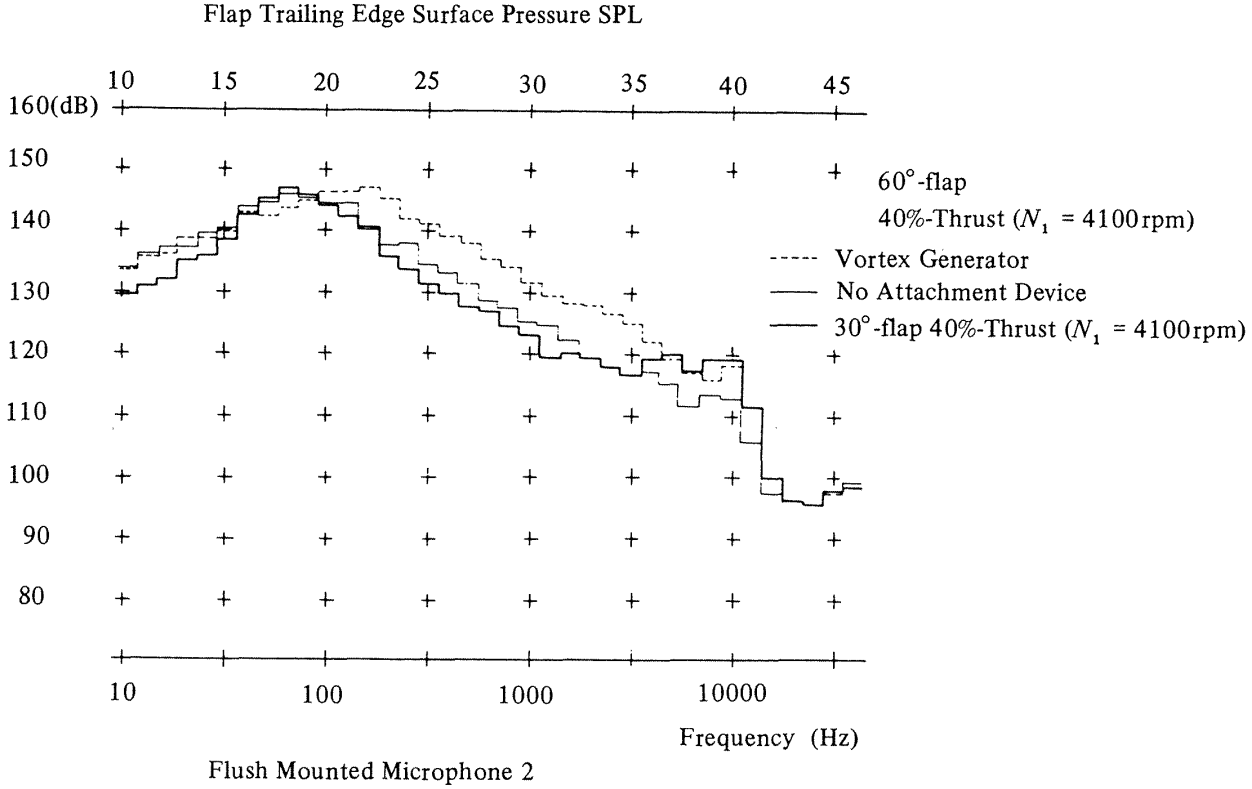

Figure 15 1/3 Octave-band spectra at flush mounted microphone 2

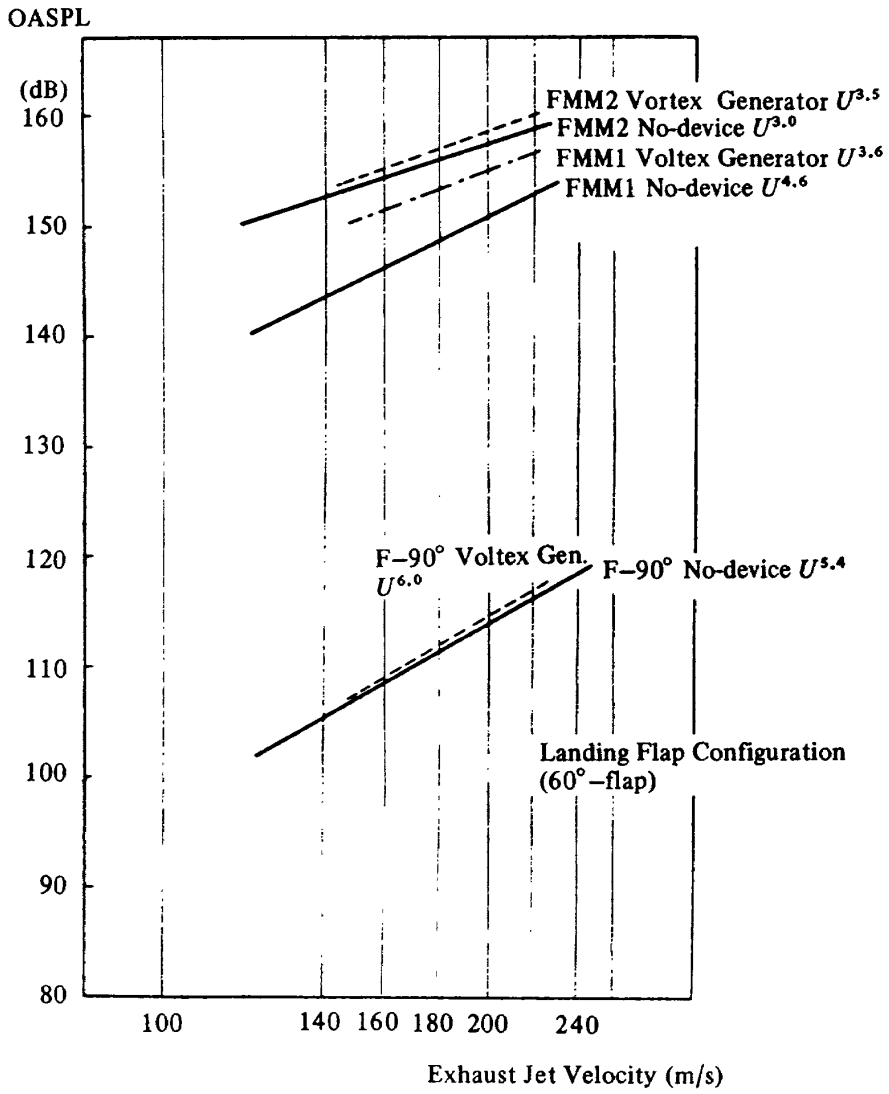

Figure 16 Overall sound pressure level dependence on exhaust velocity for landing flap configuration $\delta_f = 60°$

Noise spectral level increase at mid-frequency ranges by Vortex Generators will significantly affect the noise level when it is calculated in terms of Perceived Noise Level (PNL).

On a reduction of edge noise, several techniques such as slot secondary blowing flap at trailing edge or acoustically treated trailing edge flaps are applicable. However, on the basis of total reduction in PNL, low-frequency edge noise reductions may be less important because of Noy-weighted factors, compared with mid-frequency noise increase by the flow attachment device as found in the case of Vortex Generators. To reduce noise from the USB propulsive-lift configuration, it is necessary to optimize the powered lift system. Basically such the system optimization is acquired, in view of noise generation mechanisms, by the system that will bring about efficient powered lift with aerodynamically cleaner flow deflection. With these in mind, we have been developing the USB propulsive-lift system characterized by Side Fences[26] as a solution to this system optimization concept.

The aerodynamic characteristics of Side Fences are discussed in references of (27) ~ (29) in details.

1/3 Octave-band spectrum and lift force for the case of the USB landing flap configuration with Side Fences installed, engine thrust approximately 40 percent, at the direction Flyover Plane

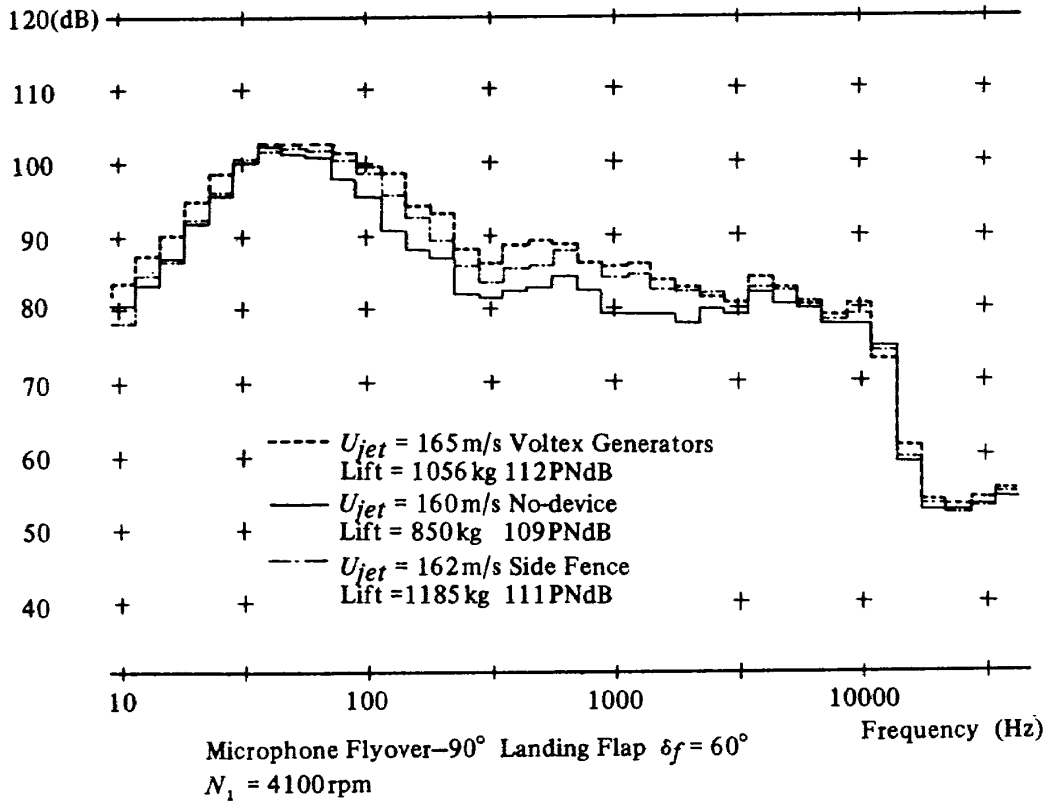

Figure 17 1/3 Octave-band spectra and lift force for the case of landing flap configuration at engine thrust 40% at the direction below the wing

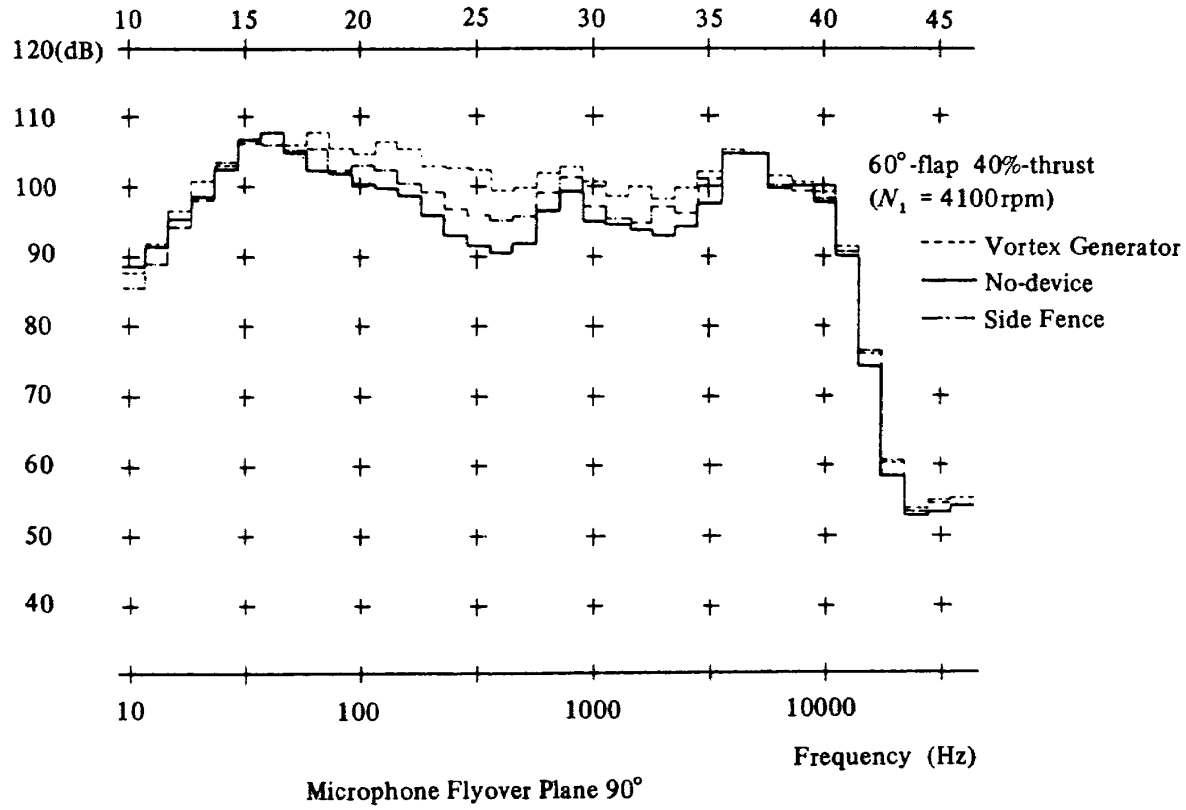

Figure 18 Effect of attachment device on 1/3 Octabe-band SPL spectra for the case landing flap configuration

-90° were presented in Figure 17, compared with the cases of Vortex Generators and no-device. (Figure 18 at the direction Flyover Plane $+90^\circ$)

The powered lift force attained by Side Fences installed USB propulsive configuration system was about 12% higher with lower noise level, compared with the case of Vortex Generators, and about 40% higher with 1.6PNdB in excess compared with no-device case (the exhaust flow being separated at after flap).

Directivity patterns of the far-field noise in OASPL and in PNL for the respective case were presented in Figure 19. (Differences between PNL and OASPL may be thought as a measure of engine noise contributions to overall noil, i.e. at the direction above the wing, high-frequency engine noise were more contributive than at the

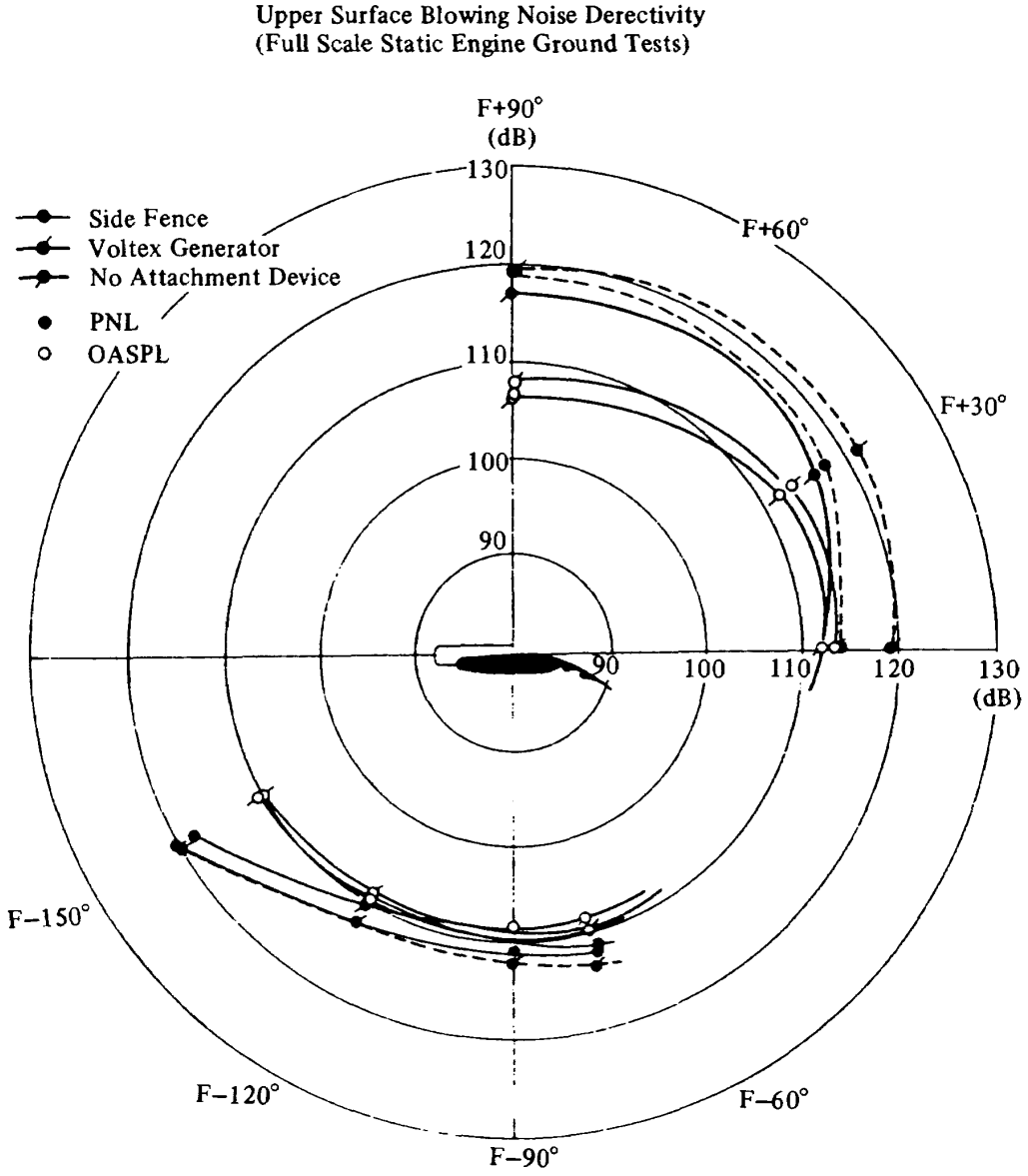

Figure 19 Directivity patterns of far-field noise in OASPL and Perceived Noise Level (PNL) for landing flap configuration at 40% thrust power

direction below the wing, and these spectral levels were highly Noy-weighted in PNL calculations and hence the difference became large, whereas at the direction below the wing, radiated noise being predominated by low-frequency spectral levels, the difference was comparatively small.)

Perceived Noise Level at the direction below the wing was approximately 4PNdB lower and 8PNdB lower than the level of engine alone case and the level at the direction above the wing respectively.

Spectral differences between the cases of Side Fences and Vortex Generators in Figures 17 and 18 at mid-frequencies are seen in Figure 19 to have affected differences of approximately 3, 5 and 1 dB in PNL at the directions Flyover +90°, 0° and −90° deg. respectively.

CONCLUDING REMARKS

The acoustic characteristics of the external upper surface blowing propulsive-lift configuration were studied experimentally using the FJR710 turbofan engine and USB wing/flap assembly. Based upon the extensive experimental noise data and the morphology of the basic theoretical studies, we have attempted to categorize noise generating mechanisms and noise source locations related to USB propulsive-lift system configurations. The main conclusions concerning the acoustic characteristics of USB propulsive-lift system are summarized as follows:

1) Engine exhaust velocity exponents of radiating sound intensity level from USB propulsive-lift configurations varied approximately as U^5_{jet} at the direction below the wing.
2) Spectral low-frequency noise in the direction below the wing was the principal contribution of jet/flap trailing edge interaction noise.
3) Normalized SPL spectral densities have similarity in form in the low Strouhal number ranges, which insure the prediction of the low-frequency noise of actual USB propulsive-lift configurations from the small-scale cold flow model analysis.
4) USB propulsive-lift system with the installation of side fences was thought to be a promising concept for quiet STOL configurations.
5) Overall fluctuating pressure levels on wing/flap surface exceeded 160dB for the cases of landing flap configuration at 60% engine power rate and takeoff flap configuration at 90% engine power rate.
6) Some of the aft-radiated turbofan engine noise was shielded by the USB wing/flap. Perceived noise level at the direction below the wing was approximately 4PNdB lower than the level of turbofan engine alone at 40% engine power rate.

ACKNOWLEDGEMENT

This research was carried out as a part of the Research Project of Fanjet STOL Aircraft.

APPENDIX I
CLASSIFICATION OF USB NOISE GENERATION MECHANISMS

The USB powered lift system noise differs in its fundamental aeroacoustic mechanisms which depend upon its configuration geometries. Based upon the extensive experimental noise data as will be discussed in the later chapters and the morphology of the basic theoretical studies[4]-[25], noise-generating mechanisms and noise source locations related to USB powered lift system are hypothetically summarized:

Related noise were thought to be attributed by four primary sources being Category I to Category IV as illustrated in the Figure 5. [Category I – Entropy Noise, Category II – Jet/Wall Jet Mixing Noise, Category III – Jet Scrubbing Noise, Category IV – Trailing Edge Noise.] Turbofan engine internal noise is regarded as not peculiar to USB system configurations and thus will not discuss in any detail.

The Category I is classified as Entropy Noise. In the environment of the external upper surface blowing propulsive lift configuration, main wing and USB flap surfaces are heated by core exhaust hot jet which have passed through combustion process. Under these USB environments, a fluid field being turbulent, or the rigit surface itself undergoes slightly oscillations in position, thermal diffusion from a heated surface to the surrounding fluid is then unsteady and produces monopole-type noise. The inhomogeneous wave equation can be written in terms of the rate of heat addition Q and density fluctuation[22] $\phi = (\rho - \rho_0)$, i.e.,

$$\frac{\partial^2 \phi}{\partial t^2} - C^2{}_0 \frac{\partial^2 \phi}{\partial x_i{}^2} = \frac{1}{C_p T_0} \frac{\partial Q}{\partial t} \qquad \text{(A.1)}$$

the solution of (A.1) reduced to,

$$4\pi C^2{}_0 (\rho - \rho_0) \sim \frac{x_i}{x^2 C_0} \int_\Sigma \frac{\partial f_i}{\partial t}(\chi, t - \frac{r}{C_0}) d\Sigma(\chi) + \frac{1}{x} \int_\Sigma \frac{\partial}{\partial t} \frac{1}{c_p T_0} Q(\chi, t - \frac{r}{C_0}) \, d\Sigma(\chi) \qquad \text{(A.2)}$$

where f_i is the force exerted by the surface on the fluid. The 1st term represents noise Category III and 2nd term, Category I. Although there would occur certain cases where unsteady heat diffusion effects overwhelm a dipole noise, i.e., lower enough flow Mach number and higher source temperature, it was not possible to think of a significant practical situation where Category I noise dominated Category III for USB configurations. Category II is defined as Jet Mixing/Wall Jet Mixing Noise radiated from exhaust jet before/after impinging to the wing and flap surfaces. As will be discussed, the related noise generation process itself is not greatly modified by the presence of the surfaces, however the solid boundary significantly modifies its radiation patterns.

Theoretical analysis estimating the intensity of noise from Category II could be referred from Lighthill who considered the exact equations of motion of a fluid under no external forces and compared the equations with the equations of sound propagation in a medium at rest. From the Momentum equation and the Continuity equation, Lighthill[8] derived the inhomogeneous wave equation in the form of (A.3),

$$\frac{\partial^2 \rho(x,t)}{\partial t^2} - C_0{}^2 \nabla^2 \rho(x,t) = \frac{\partial^2 T_{ij}}{\partial x_i \partial x_j} \qquad \text{(A.3)}$$

$$T_{ij} = \rho u_i u_j + \delta_{ij} (p - C_0{}^2 \rho) - e_{ij}$$

$$e_{ij} = \mu \left[\frac{\partial u_i}{\partial x_j} + \frac{\partial u_j}{\partial x_i} - \frac{2}{3} \delta_{ij} \frac{\partial u_k}{\partial x_k} \right]$$

where e_{ij} is viscous stress tensor and C_0 is the speed of sound in fluid at rest. Physically Lighthill's equation can be interpreted that sound is generated by a fluid flow exactly as in a uniform

medium at rest which is acted upon by externally applied fluctuating stresses.

The general solution to Lighthill's type inhomogeneous wave equation is known (Stratton[9]);

$$\rho - \rho_0 = \frac{1}{4\pi C_0^2}\iiint \frac{\partial^2 \perp_{ij}}{\partial x_i \partial x_j}\frac{d\chi}{|x-\chi|} + \frac{1}{4\pi}\iint\left[\frac{1}{\xi}\frac{\partial \rho}{\partial \eta} + \frac{1}{\xi^2}\frac{\partial \xi}{\partial \eta}\rho + \frac{1}{C_0 \xi}\frac{\partial \xi \partial \rho}{\partial \eta \partial t}\right] dS(\chi)$$

$$\xi = |x-\chi| \qquad \text{(A.4)}$$

where all the quantities $\partial^2 T_{ij}/\partial x_i \partial x_j$, ρ, $\partial\rho/\partial t$, $\partial\rho/\partial\eta$ are taken at retarted time $t-\xi/C_0$ and η takes the outward normal from the fluid. In the absence of solid boundaries, equation (A.4) reduces to the retarded potential solution since the surface integral vanishes and only the volume integral remains.

Expressing the quardrupole field as four separate source fields which come infinitely close together, then the equation (A.4) can be written in the alternative form, i.e.

$$\rho - \rho_0 = \frac{1}{4\pi C_0^2}\frac{\partial^2}{\partial x_i \partial x_j}\iiint \frac{T_{ij}\left[\chi, t - \frac{\xi}{C_0}\right]}{\xi} d\chi \qquad \text{(A.5)}$$

If $|x|$ is assumed to be sufficiently large such that x lies in the far-field of four quadrupoles, i.e. at least $|x|$ being a few acoustic wavelength and furthermore if $|x|$ is large compared with the length scale of the flow, $|x| \gg |\chi|$ then the integral of (A.5) is reduced to the following,

$$\rho - \rho_0 = \frac{1}{4\pi C_0^4}\frac{x_i x_j}{x^3}\iiint \frac{\partial^2}{\partial t^2} T_{ij}\left[\chi, t - \frac{\xi}{C_0}\right] d\chi \qquad \text{(A.6)}$$

Neglecting the entropy fluctuations and approximating the tensor T_{ij} by the Reynolds stress tensor and with the omission of the retarded-time for subsonic jet. Acoustic intensity spectrum is then estimated with the relation of (A.7),

$$I_{Jet\ Mixing} \sim \rho_0 U^8 \sin^2 2\theta T_i^4 \delta_c^2 / C_0^5 r^2 (1 - M_c \cos\theta)^5 \qquad \text{(A.7)}$$

where T_i, θ, δ_c, r and M_c represent turbulence intensity, angle of field point relative to exhaust flow direction, correlation length, far field distance and exhaust flow Mach number respectively. The scaling of (A.7) is known as Lighthill's 8th power law dependence for subsonic jet noise. As will be discussed in the later chapter, Jet alone noise data (without wing/flap) have shown to coincide with 8th power law dependence.

In the presence of solid boundaries, the required solution differs from Lighthill's solution in some respects, i.e., surface integral representing the effect on the flow itself of the solid boundaries, which will form a resultant distribution of dipole sound source at the boundaries and the sound generated by the volume distribution of quadrupoles in Lighthill's solution will be reflected and diffracted by the solid boundaries. Because of a complexity of boundary conditions for actual USB systems, no solutions have been obtained except for the simplest case.

Powell[13] et al. considered the case where the unsteady flow is bounded by an infinite plane boundary surface. For the related boundary conditions, introducing Green's function whose normal derivative vanishes on the half-plane (boundary value problem of 2nd kind). Lighthill's acoustic analogy equation of (A.3) can be reduced to the equation of (A.8) by the mirror image theory,

$$\rho - \rho_0 = \frac{1}{4\pi C^2}\left[\iiint_{\chi_{II}>0} + \iiint_{\chi_{II}<0}\right] \frac{\partial^2 G}{\partial x_i \partial x_j} T_{ij}\, d\chi + \frac{2}{4\pi C_0^2} \iint_{\substack{\chi_{II} \\ =0}} \frac{\partial G}{\partial x_i} f_i\, d\chi_I\, d\chi_{III} \quad (i = I, III) \qquad \text{(A.8)}$$

Kraichnan[11] or Powell[13] et al. showed that the strength of the surface dipole is equal to the fluctuating viscous stress and thus for inviscid flow case, the second term of the equation (A.8) vanishes and becomes,

$$\rho - \rho_0 = \frac{1}{4\pi C_0^2} \frac{\partial^2}{\partial x_i \partial x_j} \iiint \frac{\bar{T}_{ij}\left(\chi, t - \frac{\xi}{C_0}\right)}{\xi} d\chi$$

$$T_{ij} = T_{ij}(\chi_I, \chi_{II}, \chi_{III}, \tau) \quad \text{if } \chi_{II} > 0$$

$$= T^*_{ij} = (-1)^{i+j} T_{ij}(\chi_I, -\chi_{II}, \chi_{III}, \tau) \quad \text{if } \chi_{II} < 0 \qquad \text{(A.9)}$$

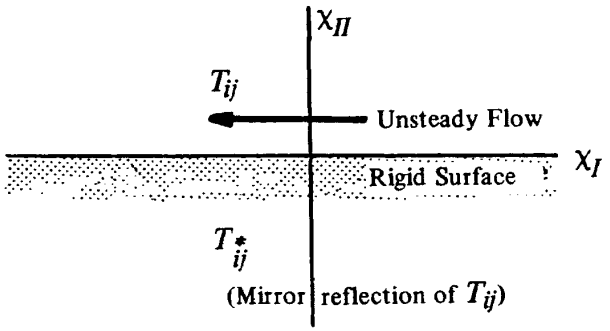

Infinite-plane Surface

The interpretation of the equation (A.9) is that [for an inviscid flow, the net effect of an infinite-plane rigid boundary can be accounted for by introducing an image distribution of volume quadrupole sources obtained by reflecting in the plane surface the volume distribution of quadrupole T_{ij}]. Thus for a given flow the solid boundary does little more than reflect the sound. These arguments were extended by Meecham[16] to more general cases when the ratio of wall jet thickness δ to the radius of surface curvature R is of small order, and has estimated that it differs by a factor of δ/R.

The wall jet leaving in the vicinity of the USB flap trailing edge where intensive mixing process being occurred, amplifies its turbulence intensity. For the estimation of the related noise generation as classified in Category IV, we refer the analysis of Ffowcs Williams and Hall[14] on the scattering half-plane problem.

Assuming the McDonald's form[17] of Green's function which has a potential-field singularity at the half-plane edge, they reduced that the edge scattered field is proportional in intensity to the fifth power of the jet velocity,

$$I_{edge} \sim \frac{\rho_0 U_{jet}{}^5 T_{int.}{}^4}{C_0{}^2 \gamma^2} \cos^2\left[\frac{\theta}{2}\right] \delta_s{}^2 \qquad \text{(A.10)}$$

where θ is angle from the forward direction.

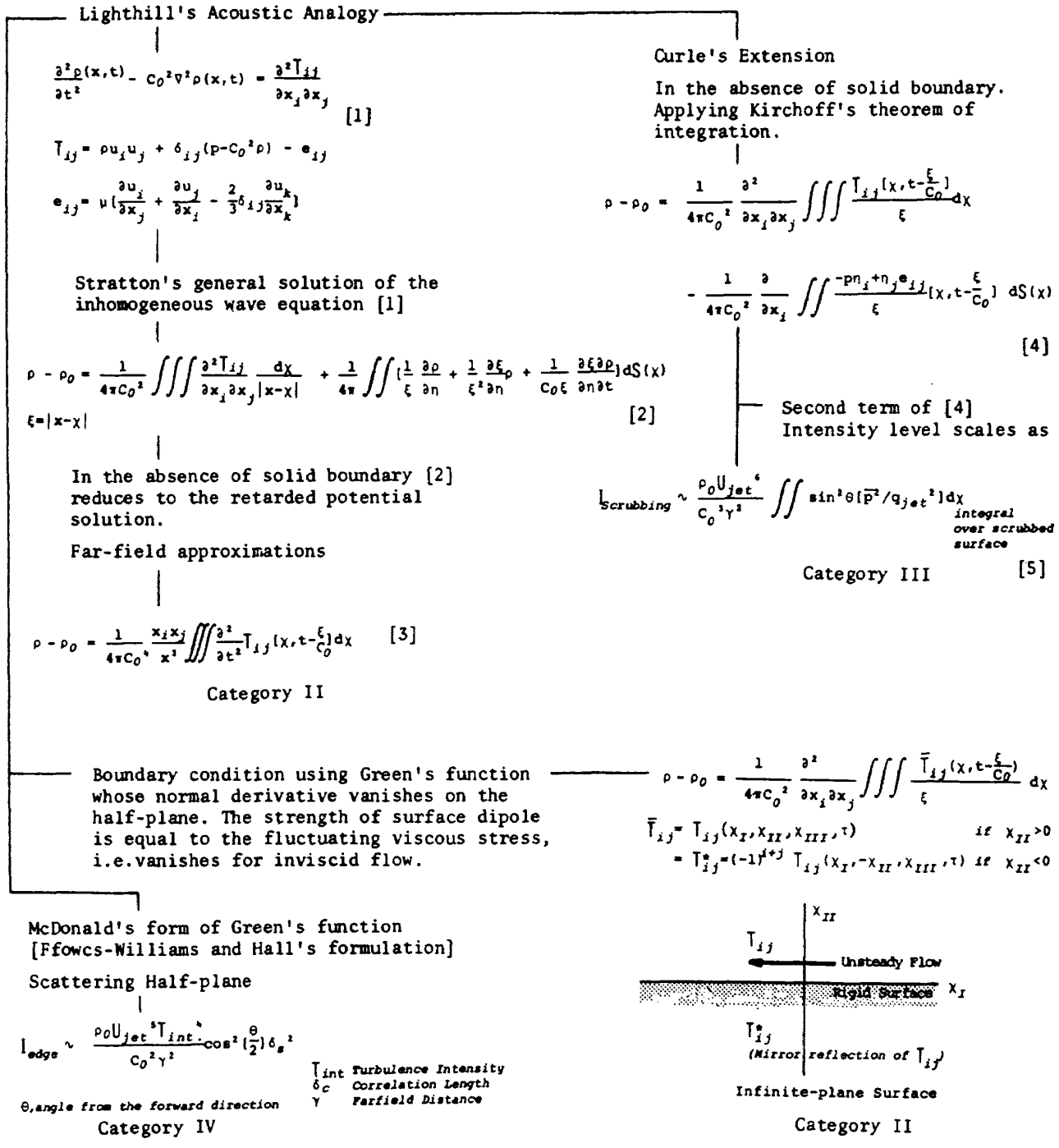

Figure A-1 Summary of Appendix I

APPENDIX II
ON THE POWERED-LIFT CONCEPTS

Considerable researches and developments have been directed over the past decade toward the powered-lift technology which is applicable to Short Take-Off and Landing (STOL) Aircraft configurations. Several STOL powered-lift concepts are generally classified into two major types, i.e., the externally blown flap type and the internally blown flap type. (cf. Figure A-2)

Typical examples of the latter concept are the Augumentor Wing and the Jet-Flap concept. The Augmentor Wing incorporates a shroud assembly over the flaps in order to create the ejector system which augments the thrust of the nozzle for the engine bleeded air by entraining additional flow. The C-8 Augmentor Wing Research Aircraft by Boeing and De Havilland was the typical case for the STOL aircraft which uses the augmentor wing concept.

Though these concepts proved to be efficient aerodynamic performances, they suffer the disadvantage that they require internal ducting which adds to the weight penalty and/or the complexity of the wing structures.

Research and development on the externally blown flap systems have come about because of the relative mechanical simplicity by eliminating internal ducting. The externally blown flap, Lower Surface Blowing concept (simply called EBF system) used with conventional pod-mounted engines was applied to McDonell-Douglas YC-15 AMST. The EBF concept uses the engine exhaust jet to produce the augmentation of lift on the wing/flaps by a direct deflected thrust vector and by flow through the flap slots which enhances the powered circulation.

Exhaust hot jets are impinging to the wing flap systems, several structural penalties due to aero-thermo-acoustic loadings and especially noise penalty have been pointed out.

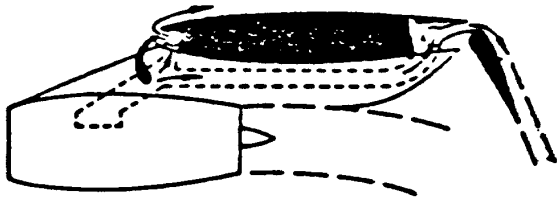

Internally Blowing Type

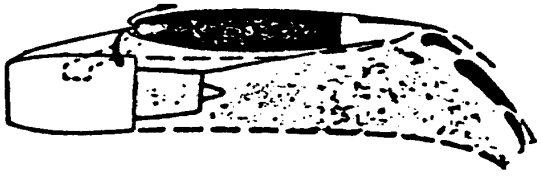

Externally Blown Flap-Lower Surface Blowing Type

EBF-Upper Surface Blowing Type

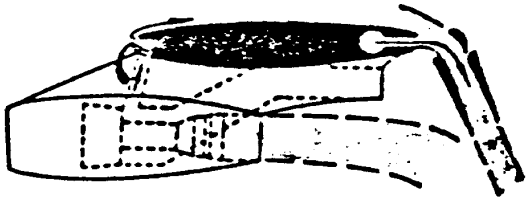

Augmentor Wing Type

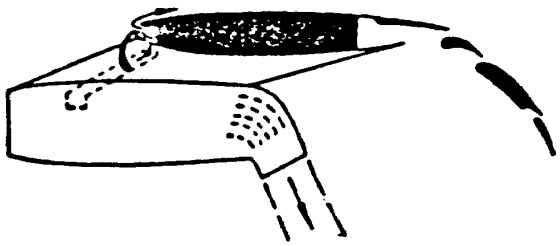

Vectored Thrust Type

Figure A-2 Powered High Lift Device

Comparing with the EBF concept, the externally Upper Surface Blowing Flap concept which achieves the powered-lift augmentation by deflecting the engine exhaust adjacent to the wing flap upper surface, have the disadvantage that USB systems need a change in engine location away from the generally accepted underslung pods, however, the preliminary noise studies showed the possibility of noise abatement because of the engine noise shielding effect by the main wing. On account of the relative mechanical simplicity and noise problems, USB type is regarded as one of the primary concepts to achieve powered high lift for STOL aircraft applications. USB concept was applied to Boeing YC-14 AMST, NASA Quiet Short Houl Research Aircraft.

National Aerospace Laboratory has been promoting the program on the research and development of Quiet STOL Aircraft as its primary project in the laboratory. (cf. Figure A-3) The object of the research program is to establish the advanced technology required in developing a powered lift STOL aircraft.

The USB concept was selected as the powered high-lift system. Main goals are the approach speed of 72 knots, including velocity margin of 20 knots, and the approach angle of $-6°$.

The research aircraft is based upon the airframe of the Kawasaki C-1 transport, with the following modifications: Replacement of the two Pratt & Whitney JT8D engines by four MITI/NAL FJR710/600S high bypass ratio turbofan engines which are installed above and far ahead of the wing leading edges in nacelles with upper surface blowing;

Installation of the wing leading edge and aileron boundary layer control (BLC) system;

Replacement of the existing inboard flaps by the USB flaps;

And installation of a digital stability and control augmentation systems.

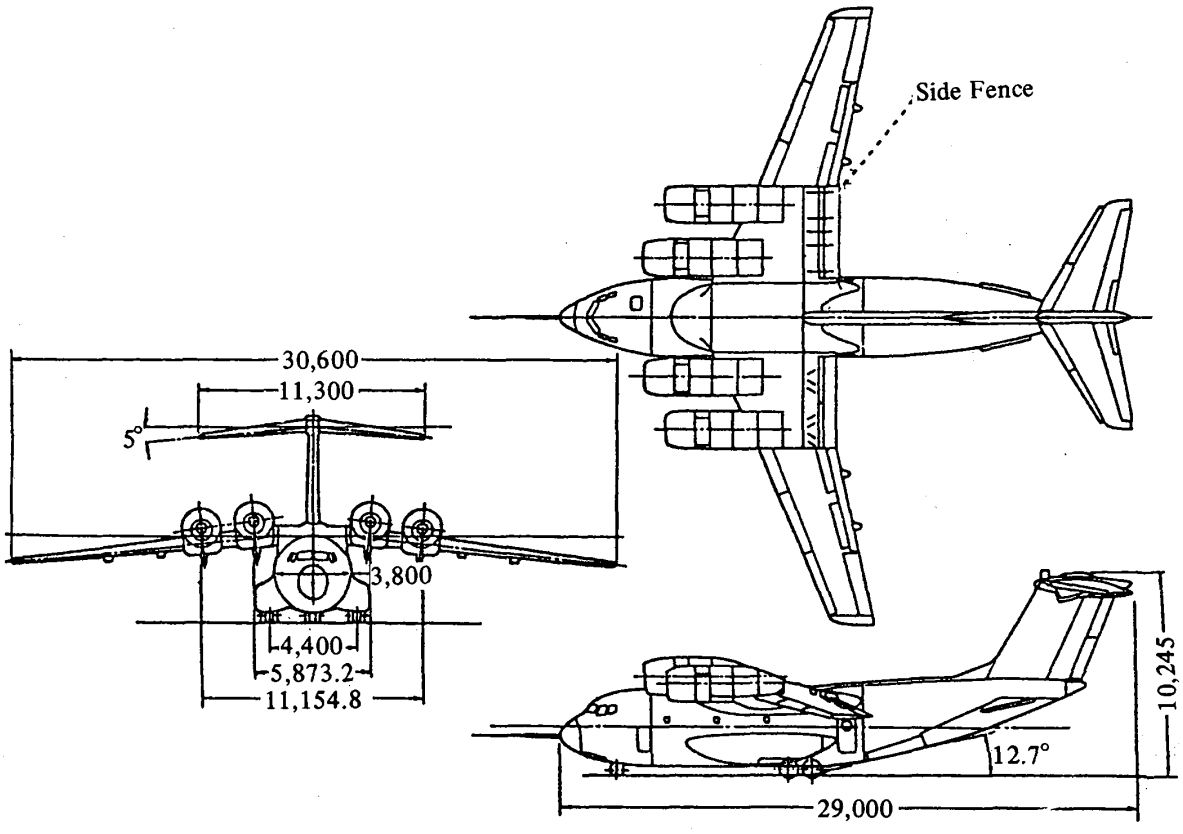

Figure A-3 General View of NAL Quiet STOL Aircraft

REFERENCES

1) Matsuki, M., "Recent Status on Research and Development of FJR710 Turbofan Engine", ASME Paper S-1, 1977.
2) B & K Microphone Product Data.
3) Watanabe, M. et. al., NAL TM-446, 1981.
4) Efowcs Williams and L. H. Hall, "Aerodynamic Sound Generated by Turbulent Flow in the Vicinity of a Scattering Half Edge", Journal of Fluid Mechanics, Vol. 40, pp. 657 ~ 670, 1970.
5) Tam, C. K. W., "Discrete Tones of Isolated Airfoils", Journal of the Acoustical Society of America, Vol. 55, pp. 1173 ~ 1177, 1974. Also AIAA Paper 75-489, 1975.
6) Paterson, W. W., Fink, M. R. and Vogt, P. G., "Vortex Noise of Isolated Airfoils", Journal of Aircraft, Vol. 10, pp. 296 ~ 302, 1973.
7) STOL Technology, NASA SP-320, 1972.
8) Lighthill, M. J., "On Sound Generated Aerodynamically I, II", Proceedings of the Royal Society, London, Vol. A211 and A222, 1952, 1962.
9) Stratton, J. A. "Electro-Magnetic Theory", McGraw Hill, New York, 1941.
10) Çurle, N. "The Influence of Solid Boundaries on Aerodynamic Sound", Proceedings of the Royal Society, London, Vol. A321, pp. 505 ~ 514, 1955.
11) Kraichnan, R. H., "Pressure Fluctuations in Turbulent Flow over a Flat Plate", Journal of the Acoustical Society of America, Vol. 28, pp. 378 ~ 390, 1956.
12) Phillips, O. M., "Aerodynamic Sound Radiated from a Turbulent Boundary Layer", Journal of the Acoustical Society of America, Vol. 30, 1958.
13) Powell, A., "Aerodynamic Noise and the Plane Boundary", Journal of the Acoustical Society of Amrica, Vol. 32, pp. 982 ~ 990, 1960.
14) Efowcs Williams, J. E. and Hawkings, D. L., "Sound Generated by Turbulence and Surfaces in Arbitrary Motion", Philosphical Transaction of Royal Society, London, Vol. A264, pp. 321 ~ 342, 1969.
15) Fink, M. R., AIAA Paper 73-1029, 1973.
16) Meecham, W. C., "Surface and Volume Sound from Boundary Layers", Journal of the Acoustical Society of America, Vol. 37, pp. 516 ~ 521, 1965.
17) McDonald, H. M., Proceedings of Mathematical Society, London, Vol. 14, pp. 410 ~ 427, 1915.
18) Maita, M., "Jet-Wing/Flap Interaction Noise from External Upper Surface Blowing Configuration", Theoretical and Applied Mechanics, Vol. 28, pp. 505 ~ 521, 1980.
19) Maita, M. et. al., Proceedings of 10th Fluid Mechanics Conference, Japan Society for Aeronautical and Space Sciences, pp. 136 ~ 139, pp. 140 ~ 143, 1978.
20) Maita, M. et. al., Proceedings of 11th Fluid Mechanics Conference, Japan Society for Aeronautical and Space Sciences, pp. 192 ~ 195, pp. 196 ~ 199, 1979.
21) Maita, M. et. al., Proceedings of 20th Conference on Aeroengines, Japan Society for Aeronautical and Space Sciences, pp. 14 ~ 17, 1980.
22) Maita, M., "Application of Stochastic Wiener-Hermite Expansion to the Problem of Aerodynamic Noise Generated by Fluctuating Entropy", AIAA Paper 80-1040, 1980.
23) Maita, M. et. al., "Acoustic Characteristics of the External USB Propulsive-Lift Configuration", Journal of Aircraft, Vol. 18, No. 8, pp. 665 ~ 701, 1981. Also ALAA Paper 80-1063, 1980.
24) Maita, M. "Some Aspects of Noise Reduction from STOL Aircraft", The Journal of the INCE of Japan, Vol. 5, No. 3, pp. 159 ~ 164. 1981.

25) Maita, M. and Shindo, S., NAL TR (To be presented)
26) Maita, M., Matsuki, M. and Torisaki, T. Patent Pending 54-148608.
27) Maita, M., "Development of the External Upper Surface Blowing Propulsive-Lift Device", AIAA Paper 80-1244, 1980.
28) Maita, M., "Effect of Side Fences on Powered-Lift Augmentation for USB Configurations", Journal of Aircraft, Vol. 19, No. 3, 1981.
29) Maita, M. et. al., NAL TR (To be presented), 1981.

TECHNICAL REPORT OF NATIONAL
AEROSPACE LABORATORY
TR-687T

航空宇宙技術研究所報告687T号（欧文）

昭和56年10月発行

発行所 航空宇宙技術研究所
東京都調布市深大寺町1880
電話武蔵野三鷹(0422)47-5911(大代表)〒182
印刷所 株式会社 東京プレス
東京都板橋区桜川2－27－12

Published by
NATIONAL AEROSPACE LABORATORY
1,880 Jindaiji, Chōfu, Tokyo
JAPAN